Acta Crystallographica Section A
**Foundations of Crystallography**
ISSN 0108-7673

Received 8 October 2009
Accepted 6 March 2010

# Combined structure-factor phase measurement and theoretical calculations for mapping of chemical bonds in GaN

**B. Jiang,[a] J. M. Zuo,[b] D. Holec,[c,d] C. J. Humphreys,[c] M. Spackman[e] and J. C. H. Spence[a]***

[a]Department of Physics, Arizona State University, Tempe, Arizona 85287, USA, [b]Department of Materials Science, University of Illinois, Urbana–Champagne 61801, USA, [c]Department of Materials Science, University of Cambridge, Cambridge CB2 3QZ, England, [d]Department of Physical Metallurgy and Materials Testing, University of Leoben, A-8700 Leoben, Austria, and [e]SBBCS, University of Western Australia, Crawley, WA 6009, Australia. Correspondence e-mail: spence@asu.edu

For non-centrosymmetric crystals, the refinement of charge-density maps requires highly accurate measurements of structure-factor phase, which can now be obtained using the extinction-free convergent-beam electron micro-diffraction method. We report here accurate low-order structure-factor phases and amplitudes for gallium nitride (GaN) in the wurtzite structure. The measurement accuracy is up to 0.1% for amplitude and 0.2° for phases. By combining these with high-order structure factors from electronic structure calculation, charge-density maps were obtained. Fine bonding features suggest that the Ga—N bonds are polar and covalent, with charge transfer from Ga to N; however, the polarity effect is extremely small.



## 1. Introduction

GaN has been extensively studied because of its usefulness for the fabrication of optoelectronic devices working in the blue–violet range and for high-frequency power devices (Paskova, 2008). The electronic and crystal structures of GaN and its alloys have been intensively studied, using both density functional theory (DFT) calculations and experimental measurement. Despite the importance of the material, good-quality single crystals have become available only recently, so that accurate measurements of the ground-state valence electron distribution have not previously been possible. The measurements we report here make it possible to evaluate the results of theoretical electronic structure calculations for the electron density. In order to avoid extinction errors which can lead to errors in X-ray measurements at low angles, we use the convergent-beam method, based on electron diffraction in a transmission electron microscope. This allows diffraction patterns to be obtained from nanometre-sized regions of a highly perfect crystal (smaller than one 'mosaic block') and an analysis which takes full account of multiple scattering.

Using elastic energy-filtered quantitative convergent-beam electron diffraction (QCBED), low-order structure-factor measurements have recently been obtained for many crystals with high precision [see Zuo (2004) for a review]. The advantage of electron diffraction is that it is more sensitive to bonding effects at low scattering angles than X-ray diffraction (Zuo, 2004). In addition, the method takes advantage of the small electron probe (smaller than a single mosaic block) to avoid extinction errors, and the ability of the transmission electron microscope to image the region used, in order to avoid defects. The 'perfect crystal' dynamical diffraction theory is applied in simulations, thereby incorporating all multiple scattering effects exactly. This method refines many parameters – structure factors (amplitude and phase, for non-centrosymmetric crystals), absorption, beam direction and sample thickness – in the multiple electron scattering calculations. It also measures the structure factors on an absolute scale. Since the bond charge distribution in non-centrosymmetric crystals influences the phase of structure factors, phase measurement is required in these crystals (Le Hénaff *et al.*, 1997). QCBED is uniquely capable of providing this information from nanoscale regions of these crystals, information that is not present in kinematic Bragg beam intensities. Phase measurement based on the multiple scattering of X-rays can provide an accuracy of about 20° (Weckert & Hümmer, 1997) which, although useful for crystal structural analysis, is insufficient for the study of bonding in non-centrosymmetric crystals, and for tests of band-structure calculations.

In this work, we report our study of wurtzite GaN by QCBED. Both amplitudes and phases of structure factors have been measured, and we have compared these with theoretical calculations based on both the local density approximation (LDA) and the generalized gradient approximation (GGA). Results show that both approximations agree

with the experimental results, with an $R$ factor of about 0.6% or a weighted $R$ factor of 0.3%. Using the measured low-order structure factors, we show the difference between experimental and theoretical charge density in the regions between atoms, where chemical bonds reside.

## 2. QCBED experimental methodology

The QCBED method provides a complete two-dimensional Bragg rocking curve, containing many points or pixels for each reflection. Each pixel corresponds to one of the many independent incident-beam directions selected from the illuminating cone. The calculation of the intensity of the convergent-beam electron diffraction (CBED) Bragg beam intensity is based on Bloch-wave solutions of Schrödinger's equation in reciprocal-lattice space (Spence & Zuo, 1992). The multiply scattered amplitude and phase are stored in each pixel of the simulated CBED discs for comparison with experimental intensities. The effect of inelastic scattering (absorption) has been included through the addition of a small imaginary component. This results in a non-Hermitian eigenvalue problem. For a parallel-sided slab of crystal traversed by an electron beam inclined to the surface normal **n** we obtain

$$\frac{2KS_gB_g^{(j)}}{1+g_n/K_n}+\sum_h\frac{B_h^{(j)}U_{g-h}}{(1+g_n/K_n)^{1/2}(1+h_n/K_n)^{1/2}}=2K_n\gamma^{(j)}B_g^{(j)}, \tag{1}$$

where $U_g$ is a complex electron structure factor, **K** is the electron wavevector and the reciprocal-lattice vector is **g**. Here $g_n=\mathbf{g}\cdot\mathbf{n}$, $K_n=\mathbf{K}\cdot\mathbf{n}$, with $S_g$ the excitation error. For an eigenvalue $\gamma^{(j)}$, eigenvector $B_g^{(j)}=[1+(g_n/K_n)]^{1/2}C_g^{(j)}$ [$C_g^{(j)}$ is the Fourier coefficient of a Bloch wave]. Starting values for the $U_g$'s are calculated using a neutral atom model, calculated using the Dirac–Fock method (Doyle & Turner, 1968), and the low orders are refined. This equation is solved numerically and the intensity at the point $(K_x, K_y)$ in each disc **g** of the CBED pattern is given by

$$I_g(K_x,K_y)=\left|\sum_{i=1}^{n}C_0^{i-1}C_g^i\exp(2\pi i\gamma^i t)\right|^2, \tag{2}$$

where $C_0^{i-1}$, $C_g^{(j)}$, $\gamma^{(j)}$ are functions of the incident electron-beam direction $(K_x, K_y)$. They are obtained by diagonalizing equation (1). $C_0^{i-1}$ is the first column of the inverse eigenvector matrix and $t$ is the crystal thickness. The QCBED refinement is automated by defining a goodness of fit (GOF) parameter and using numerical optimization routines to search while adjusting the input structure factors. A useful GOF for direct comparison of experimental and theoretical intensities in CBED discs is the Euclidean metric $\chi^2$,

$$\chi^2=\frac{1}{n-p-1}\sum_k(1/\sigma_k^2)(I_k^{\rm exp}-cI_k^{\rm theory})^2, \tag{3}$$

where $I^{\rm exp}$ and $I^{\rm theory}$ are the experimental and theoretical intensities, $n$ is the total number of experimental points, $j$ is the index of each point, and $p$ is the number of refinement parameters, including the number of refined structure factors, sample thickness and geometric parameters (incident-beam direction, pattern geometry). $\sigma$ is the variance, estimated from the charge-coupled device (CCD) detector quantum efficiency and experimental intensity (Zuo, 1998). This method has been found to be a robust refinement approach as tested in many previous experimental examples (Zuo *et al.*, 1997, 1999; Jiang, Zuo, Friis & Spence, 2003; Jiang, Zuo, Jiang *et al.*, 2003; Jiang *et al.*, 2004; Friis *et al.*, 2003) including a few cases of non-centrosymmetric crystals (Zuo *et al.*, 1989, 1993; Spackman *et al.*, 2005).

## 3. QCBED experiment

CBED patterns were collected on a Leo-912B electron microscope with an in-column Ω filter and a Gatan MSC CCD camera with 14-bit dynamical range. The specimen was cooled to 113 K. The high voltage was calibrated to be 119.60 keV by dynamical fitting of high-order Laue zone line patterns from silicon. Diffraction astigmatism was corrected using an aluminium sample until no observable astigmatism remained. CCD characteristics were measured and the point spread function of the CCD camera was deconvoluted before refinement. The GaN single crystals used for electron diffraction were grown by metal organic vapour deposition on sapphire. Transmission electron microscope samples were prepared by the wedge tripod grinding method and ion beam thinning. The sample thickness used for CBED is about 500–800 Å. CBED patterns were recorded in the systematic row orientation and used for structure-factor refinement. In this geometry, only two reflections along a line are close to the Bragg condition and strongly excited. An example of a CBED pattern for the (101) systematic row of GaN is shown in Fig. 1, with the calculated multiple scattering for best fit. In this orientation, the recorded intensities are highly sensitive to the few low-order structure factors for which the Bragg condition is nearly satisfied. Only these structure factors (one or two) are then refined; other values are calculated from the neutral-atom model. The refined electron structure factors are then converted to their X-ray structure-factor equivalents using Poisson's equation in reciprocal space, *i.e.* the Mott–Bethe formula (Spence & Zuo, 1992).

## 4. DFT calculations

DFT as implemented in the all-electron linear augmented plane waves code *Wien2k* (Blaha *et al.*, 1990) was used to calculate the 0 K ground state of GaN. A wurtzite unit cell with four atoms (two Ga and two N) at Wyckoff 2*b* positions and lattice parameters of $a = 3.1868$, $c = 5.1830$ Å and $u = 0.377$ was adopted (at 113 K; Reeber & Wang, 2000; Schulz & Thiemann, 1977). The respective muffin-tin sphere (MTS) radii for Ga and N were 1.92 and 1.65 Bohr. The $l$ expansion (azimuthal quantum number) of the non-spherical potential and charge density inside the MTSs was carried out up to $l_{\rm max} = 10$. The plane waves were expanded up to a cut-off parameter, $K_{\rm max}$, fulfilling the relation $R_{\rm MT}K_{\rm max} = 8$ where $R_{\rm MT}$ is the average radius of the MTSs. The convergency was tested.

It showed that $R_{MT}K_{max} = 8$ gives very good convergency. The maximum LM expansion is 6.6. The radial mesh points for the radial function of the local orbital are 981. The entire first Brillouin zone was sampled at 5000 $k$ points in order to obtain highly accurate results. The self-consistent iteration process was repeated until the charge density and the total energy were converged within the precision of 0.001 e and 0.0001 Ry, respectively. The exchange–correlation potential was evaluated using (i) the local spin density approximation (LSDA) (Perdew & Wang, 1992) and two parameterizations of the GGA, namely by (ii) Perdew *et al.* (1996) (GGA-PBE) and by (iii) Wu & Cohen (2006) (GGA-WC). Variations in the predictions of various approximations are the subject of the discussion in the following section. The charge density obtained was subsequently used to calculate the 0 K X-ray structure factors by applying the Fourier transform implemented in the routine *lapw3*, a part of the *Wien2k* package.

## 5. Comparison between experiment and theory

To take account of both structure-factor amplitudes and phases in the comparison between experimental and theoretical structure factors, we introduce the following metric for the $R$ factor and $\chi^2$. First, we define the standard deviation of the complex structure factor as

$$\sigma = (\sigma^{F^2} + |F|^2\sigma^{p^2})^{1/2}, \quad (4)$$

where $\sigma^F$ and $\sigma^p$ are the measured standard deviations of the structure-factor amplitude and phase (in radians), respectively; $|F|$ is the experimental structure-factor amplitude. Using the calculated standard deviation, we then calculate $\chi^2$ according to

$$\chi^2 = \frac{1}{n-1}\sum_{k=1}^{n}\frac{1}{\sigma_k^2}\left[(F_{k,x}^{e} - F_{k,x}^{t})^2 + (F_{k,y}^{e} - F_{k,y}^{t})^2\right], \quad (5)$$

where $F_{x(y)}^{e}$ and $F_{x(y)}^{t}$ are the real and imaginary components of the experimental and theoretical structure factors, respectively.

Similarly, we define the residuals ($R$ factor) and weighted residuals according to

$$R = \sum_k[(F_{k,x}^{e} - F_{k,x}^{t})^2 + (F_{k,y}^{e} - F_{k,y}^{t})^2]^{1/2} / \sum_k |F_k^{e}|, \quad (6)$$

$$R_w = \sum_k\left\{\left[(F_{k,x}^{e} - F_{k,x}^{t})^2 + (F_{k,y}^{e} - F_{k,y}^{t})^2\right]^{1/2}/\sigma_k\right\} / \sum_k(|F_k^{e}|/\sigma_k). \quad (7)$$

Using the above metrics, we calculated the residuals and weighted residuals by considering both structure-factor amplitude and phase, and the $\chi^2$ values as well (Table 1). The calculated residuals and weighted residuals are similar. It is noticed that the major contribution to $\chi^2$ is from the $(\bar{1}0\bar{1})$ reflection; the difference between the measured phase and its theoretical value is several times the standard deviation. The $\chi^2$ values calculated without the $(\bar{1}0\bar{1})$ structure factor are also listed in Table 1.

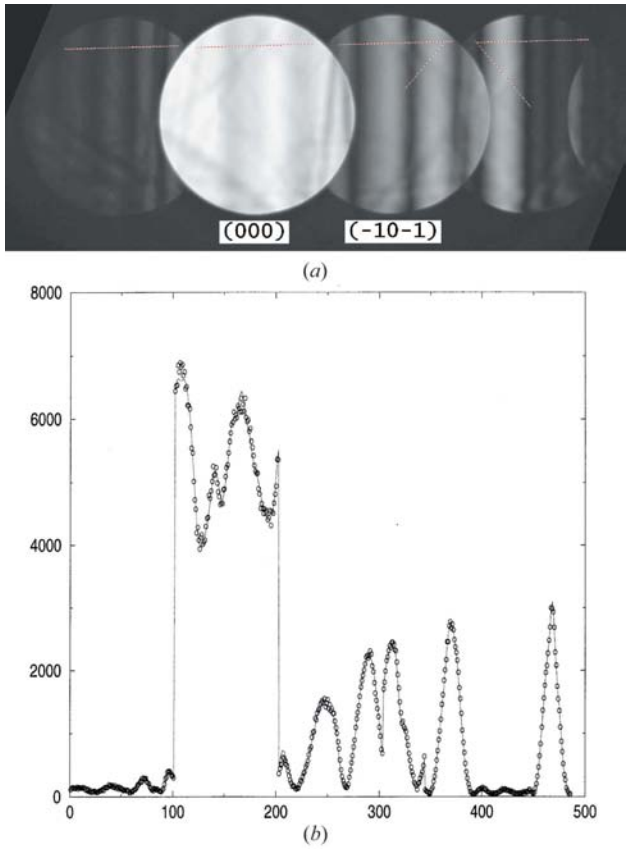


**Figure 1**
This figure shows an example of the electron structure-factor refinement for the GaN crystal for the $(\bar{1}0\bar{1})$ $(\bar{2}0\bar{2})$ systematic row. (*a*) Experimental recorded and deconvoluted CBED pattern (Zuo, 1998). The experimental temperature is 113 K. (*b*) Best fit along the line indicated in (*a*). The $x$ axis is pixels, displayed sequentially, and the $y$ axis is counts. The circles are experimental data and the lines are theoretical calculations. The overall GOF is $\chi^2 = 2.8$.

## 6. Results and discussion

A total of 50 CBED patterns for GaN were refined. They provided the 11 structure factors for GaN listed in Table 2. Four of the phases are fixed by symmetry, the remainder were measured. The accuracy in the X-ray structure factors derived from these electron diffraction measurements is at best 0.1% for amplitudes and 0.2° for phases. The smaller the scattering angle, the more accurate is the measured structure factor. The accuracy decreases for high scattering angles. The measured electron structure factors and converted X-ray structure factors are listed in Table 1. Note that the experimental standard deviation for the converted X-ray structure factor is normally lower than 0.5%. All the phase measurements are within ±0.5°. This accurate measurement of phase gives additional information on Ga—N bonding, unavailable by other methods. We note that the overall fit for structure-factor amplitude and phase between our DFT calculation (in particular, using the LSDA parameterization for the exchange and correlation term) and electron diffraction is within $\sigma$ for most of the beams except the $(\bar{1}0\bar{1})$ reflection. Thus we conclude that DFT theory gives a good description of the ground-state

**Table 1**
X-ray structure factors converted from electron diffraction values at 0 K using the Mott formula for static X-ray structure factors.

Note that the standard deviation of these X-ray structure factors is normally within 0.3%, and at best 0.1% for amplitudes and 0.2° for phases [see the $(\bar{1}0\bar{1})$ reflection]. The phase measurements are within 0.5°. The experimental measurements listed in Table 2 are converted to X-ray structure factors at 0 K. Crystal parameters and temperature factors used for this conversion are taken from Reeber & Wang (2000) and Schulz & Thiemann (1977). Crystal parameters used for 113 K: $a$ = 3.1868, $c$ = 5.1830 Å and $u$ = 0.377. The temperature factors are interpolated from room temperature to 113 K using a Debye model (Coppens, 1997). Temperature factors used for 113 K: Ga $U_{11}$ = 0.00248, $U_{33}$ = 0.00143; N $U_{11}$ = 0.00433, $U_{33}$ = 0.00195. The standard deviation was calculated based on the standard deviation of the electron structure factor. $\chi^2$, residual and weighted residual are calculated according to equations (5), (6) and (7).

| | CBED experiments (0 K) | | DFT theory (0 K) | | | | | |
|---|---|---|---|---|---|---|---|---|
| | | | LSDA | | GGA-PBE | | GGA-WC | |
| (*hkl*) | $\lvert F\rvert$ (e unit cell$^{-1}$) | $\varphi$ (°) | $\lvert F\rvert$ (e unit cell$^{-1}$) | $\varphi$ (°) | $\lvert F\rvert$ (e unit cell$^{-1}$) | $\varphi$ (°) | $\lvert F\rvert$ (e unit cell$^{-1}$) | $\varphi$ (°) |
| (100) | 30.79 (7) | 180 | 30.83 | 180 | 30.85 | 180 | 30.83 | 180 |
| $(00\bar{2})$ | 51.77 (11) | 11.0 (2) | 51.54 | 11.22 | 51.56 | 11.28 | 51.54 | 11.24 |
| $(\bar{1}0\bar{1})$ | 37.28 (3) | 81.7 (1) | 37.30 | 81.08 | 37.28 | 81.03 | 37.29 | 81.06 |
| $(\bar{1}0\bar{2})$ | 23.05 (1) | −170.7 (6) | 23.00 | −170.63 | 23.01 | −170.60 | 23.00 | −170.62 |
| (110) | 48.09 (1) | 0 | 48.06 | 0 | 48.10 | 0 | 48.08 | 0 |
| $(\bar{1}0\bar{3})$ | 38.23 (14) | 84.7 (1.5) | 38.17 | 84.63 | 38.21 | 84.63 | 38.19 | 84.63 |
| $(\bar{2}00)$ | 22.3 (4) | 180 | 21.89 | 180 | 21.91 | 180 | 21.90 | 180 |
| $(00\bar{4})$ | 32.2 (4) | 0.6 (2) | 32.43 | 0.80 | 32.47 | 0.78 | 32.46 | 0.79 |
| $(\bar{2}0\bar{2})$ | 17.8 (2) | −170.8 (8) | 18.06 | −172.92 | 18.08 | −172.93 | 18.07 | −172.93 |
| $(\bar{2}04)$ | 12.8 (9) | 179.6 (1.7) | 12.82 | 179.66 | 12.84 | 179.65 | 12.83 | 179.66 |
| (220) | 27.9 (2) | 0 | 28.21 | 0 | 28.21 | 0 | 28.21 | 0 |
| Residual (%) (11 beams) | | | $R$ = 0.78 | | $R$ = 0.83 | | $R$ = 0.81 | |
| Weighted residual (%) (11 beams) | | | $R_w$ = 0.22 | | $R_w$ = 0.24 | | $R_w$ = 0.23 | |
| $\chi^2$ (11 beams) | | | $\chi^2$ = 4.0 | | $\chi^2$ = 4.6 | | $\chi^2$ = 4.2 | |
| $\chi^2$ [without $(\bar{1}0\bar{1})$] | | | $\chi^2$ = 1.23 | | $\chi^2$ = 1.32 | | $\chi^2$ = 1.26 | |

charge density of GaN crystals. The GGA-WC-based structure factors lie always between the values of GGA-PBE and LSDA calculations. Optimized lattice parameters were also used to calculate structure factors. After scaling these structure factors according to experimental lattice parameters, we obtained a similar result.

These results are demonstrated graphically in Fig. 2, which shows the resulting density-map sections and projections. Fig. 2(*b*) shows the theoretical electron-density deformation map based on our GGA-PBE calculation, without resolution limits. Fig. 2(*c*) shows the electron-density difference between our experimental map and theoretical calculations using only eight complex structure factors in Table 1 [up to the (004) reflection]. It is obtained using the Fourier transform of $(F_{\rm exp} - F_{\rm band\ theory})$. This shows a very small difference, due to the good agreement between experimental measurements and band-theory calculations. The resolution is limited by the highest-order reflection (004), which is 1.30 Å. Fig. 2(*a*) is obtained using Fig. 2(*b*) plus Fig. 2(*c*), and can therefore be interpreted as an experimental charge-density deformation map which uses band-theory calculations for the high-order reflections and eight low-order experimental measurements.

In summary, the convergent-beam electron diffraction method has been applied to the measurement of structure-factor phases and amplitudes. Structure factors have been measured for the GaN semiconductor for the first time with high precision. These structure-factor phase measurements could otherwise only be provided by the *Pendellösung* X-ray method, which requires a large single crystal of GaN, which is not currently available. Charge-density maps have been obtained for GaN by combining CBED and band-structure calculations. Fig. 2(*a*) clearly shows the charge transfer from the Ga atom to the N atom. There is a high charge concentration between Ga and N atoms. The peak value is 0.15 e Å$^3$. These kinds of features suggest the presence of a polar Ga—N covalent bond. Bader analysis (Bader, 1990) was also performed by *Wien2k* to estimate the charge transfer between Ga and N atoms. Using the GGA-PBE approximation, the Ga basin charge is calculated to be 29.43 e, and the N basin charge 8.57 e. With the neutral-atom model, we estimated the Ga basin charge to be 29.797 e and the N basin charge 8.179 e using the *VALRAY* program (Stewart *et al.*, 2000). Bader analysis suggests there is a charge transfer from Ga to N, consistent with our experimental observations. However, we emphasize how small this effect is, as seen by the very small

**Table 2**
The measured electron structure factors $U_g$ at 113 K.

The high tension of the transmission electron microscope (TEM) was calibrated at 119.60 kV. The TEM sample temperature takes into account a 6 K difference between the sample and holder temperatures (Jiang, Zuo, Jiang *et al.*, 2003).

| | CBED measurements | |
|---|---|---|
| (*hkl*) | $U_g$ modulus (Å$^{-2}$) | $U_g$ phase (°) |
| (100) | 0.0449 (4) | 180 |
| $(00\bar{2})$ | 0.0676 (4) | 19.8 (8) |
| $(\bar{1}0\bar{1})$ | 0.0422 (1) | 110.6 (4) |
| $(\bar{1}0\bar{2})$ | 0.0264 (1) | −155 (3) |
| (110) | 0.05708 (3) | 0 |
| $(\bar{1}0\bar{3})$ | 0.0406 (3) | 79 (1) |
| $(\bar{2}00)$ | 0.0239 (6) | 180 |
| (004) | 0.0210 (6) | −1.5 (3) |
| $(\bar{2}0\bar{2})$ | 0.0169 (2) | −163 (1) |
| $(\bar{2}04)$ | 0.008020 (1) | 175 (4) |
| (220) | 0.0230 (1) | 0 |

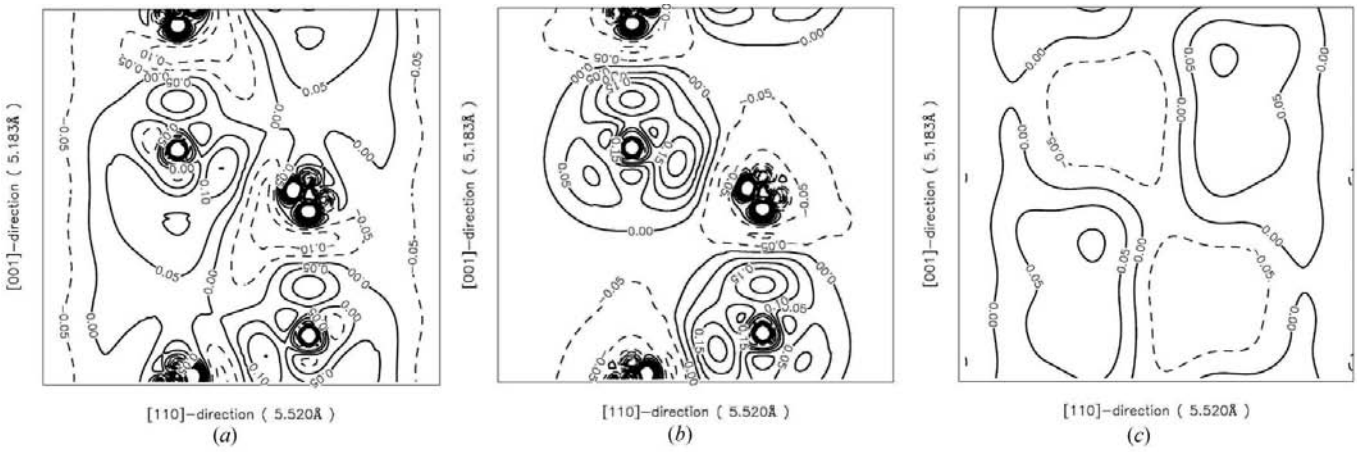


**Figure 2**
(*a*) Approximation of the experimental deformation charge-density map for GaN. It is obtained from the theoretical charge-density map (Fig. 2*b*) plus the map of Fig. 2(*c*). The result shown uses experiments for the low eight orders and theory for the high orders. (*b*) Theoretical valence electron deformation charge-density map for GaN from DFT (GGA-PBE) calculations. Reading down the figures from the top, the atoms are Ga, N, Ga, N, Ga. The unit of the contour level is e $Å^{-3}$. (This deformation map is obtained from the theoretical valence charge density minus the valence charge density of the neutral atom model. The *x* axis is along the [110] direction of the GaN crystal with 5.520 Å length, the *y* axis is along the [001] direction of the GaN crystal with 5.183 Å length.) (*c*). Experimental density map minus calculated map, both limited to eight complex structure factors, and using measured phases. Because of the good agreement between theory and experiment, the map is close to zero. Atom positions of Ga and N are also labeled in the map.

differences between our DFT calculations and a spherical-atom model for both structure-factor amplitudes and phases. It remains to be determined, based partly on the availability of suitable crystals, whether these measurements can be combined with X-ray structure-factor measurements for high orders in a multipole analysis which incorporates refinement of phases (Spackman *et al.*, 2005; Coppens, 1997) to provide a clearer picture of the polar bond and other ground-state properties of this important material.

This research was supported by DOE award Nos. DE-FG03-02ER45996 (to JCHS) and DEFG02-01ER45923 (to JMZ). The experiments were performed at the John Cowley EM Center at ASU. DH acknowledges the EU project PARSEM (contract No. MRTN-CT-2004-005583) and the START Program (Y371) of the Austrian Science Fund (FWF). We also acknowledge the helpful comments from one referee on the DFT calculations.

## References

Bader, R. F. W. (1990). *Atoms in Molecules – a Quantum Theory*. Oxford University Press.
Blaha, P., Schwarz, K., Madsen, G., Kvasnicka, D. & Luitz, J. (1990). *Comput. Phys. Commun.* **59**, 399–415.
Coppens, P. (1997). *Charge Densities and Chemical Bonding.* New York: Oxford University Press.
Doyle, P. A. & Turner, P. S. (1968). *Acta Cryst.* A**24**, 390–397.
Friis, J., Madsen, G. H. K., Larsen, F. K., Jiang, B., Martinsen, K. & Holmestad, R. J. (2003). *Chem. Phys.* **119**, 11359–11366.
Jiang, B., Friis, J., O'Keeffe, M. & Spence, J. C. H. (2004). *Phys. Rev. B*, **69**, 245110–245120.
Jiang, B., Zuo, J. M., Friis, J. & Spence, J. C. H. (2003). *Microsc. Microanal.* **9**, 457–476.
Jiang, B., Zuo, J. M., Jiang, N., O'Keeffe, M. & Spence, J. C. H. (2003). *Acta Cryst.* A**59**, 341–350.
Le Hénaff, C., Hansen, N. K., Protas, J. & Marnier, G. (1997). *Acta Cryst.* B**53**, 870–879.
Paskova, T. (2008). *Phys. Status Solidi B*, **245**, 1011–1025.
Perdew, J. P., Burke, K. & Ernzerhof, M. (1996). *Phys. Rev. Lett.* **77**, 3865–3868.
Perdew, J. P. & Wang, Y. (1992). *Phys. Rev. B*, **45**, 13244–13251.
Reeber, R. R. & Wang, K. (2000). *J. Mater. Res.* **15**, 40–44.
Schulz, H. & Thiemann, K. H. (1977). *Solid State Commun.* **23**, 815–818.
Spackman, M., Jiang, B., Groy, T., He, H., Whitten, A. & Spence, J. C. H. (2005). *Phys. Rev. Lett.* **95**, 085502.
Spence, J. C. H. & Zuo, J. M. (1992). *Electron Microdiffraction.* New York: Plenum Press.
Stewart, R. F., Spackman, M. A. & Flensburg, C. (2000). *VALRAY User's Manual.* Carnegie Mellon University, Pittsburgh, PA, USA, and University of Copenhagen, Denmark.
Weckert, E. & Hümmer, K. (1997). *Acta Cryst.* A**53**, 108–143.
Wu, Z. & Cohen, R. (2006). *Phys. Rev. B*, **73**, 235116.
Zuo, J. M. (1998). *Mater. Trans. JIM*, **39**, 938–946.
Zuo, J. M. (2004). *Rep. Prog. Phys.* **67**, 2053–2129.
Zuo, J. M., Kim, M., O'Keeffe, M. & Spence, J. C. H. (1999). *Nature* (*London*), **401**, 49–52.
Zuo, J. M., O'Keeffe, M., Rez, P. & Spence, J. C. H. (1997). *Phys. Rev. Lett.* **78**, 4777–4780.
Zuo, J. M., Spence, J. C. H., Downs, J. & Mayer, J. (1993). *Acta Cryst.* A**49**, 422–429.
Zuo, J. M., Spence, J. C. H. & Hoier, R. (1989). *Phys. Rev. Lett.* **62**, 547–550.